Ab Initio Study of Bonding between Nucleophilic Species and the Nitroso Group

Gabriel da Silva,† Eric M. Kennedy,* and Bogdan Z. Dlugogorski

Process Safety and Environment Protection Research Group, School of Engineering, The University of Newcastle, Callaghan, NSW 2308, Australia

Received: August 1, 2005; In Final Form: November 13, 2006

The bonding between anionic nucleophiles and the nitroso group has been studied in the common nitrosating agents nitroso chloride (ONCl), nitroso bromide (ONBr), nitroso thiocyanate (ONSCN), and dinitrogen trioxide (N_2O_3) in aqueous solution. A variety of theoretical methods were employed, including ab initio, density functional theory (DFT), and composite theoretical techniques, with solvent effects described using the polarizable continuum model (PCM). Experimental nitroso bond heterolytic dissociation free energies were accurately reproduced with a number of composite theoretical methods, the most successful being CBS-Q and G2MP2, with average errors of 3.1 and 3.4 kJ mol^{-1}, respectively. Using the MP2 and B3LYP methods, calculations were made with correlation consistent basis sets up to quadruple-ζ, extrapolated to the complete basis set (CBS) limit. The MP2/CBS calculations were accurate to around 10 kJ mol^{-1}, while the B3LYP/CBS calculations routinely overpredicted experimental bond free energies by ca. 40 kJ mol^{-1}. It is therefore highly recommended that B3LYP energies are not used for nitroso compounds, although other results demonstrate that the B3LYP method provides a good account of nitroso compound geometries, frequencies, and entropies. Single-point CBS energy calculations using MP2/aug-cc-pVQZ geometries and frequencies showed that the MP4(SDTQ) and QCISD(T) methods provide a slight improvement over MP2 at the CBS limit, although the inclusion of triple excitations is necessary to achieve this improvement in accuracy. Enthalpy−entropy compensation was also discovered, with an average isoequilibrium temperature of 825 K. This relatively large isoequilibrium temperature indicates that enthalpic effects dominate over entropic ones.

Introduction

Reactions involving nitroso group transfer are of wide interest across many areas of chemistry. These reactions are significant because of their role in the in vivo production of nitric oxide, an important physiological regulator,[1] and because of their ability to generate potentially carcinogenic *N*-nitrosamines.[2] Nitrosation reactions are also of relevance to, for example, the petroleum, chemical, and explosives industries.[3] Accordingly, there is considerable interest in both the thermodynamics and the kinetics of nitroso transfer reactions. We are now beginning to gain greater insight into the factors that contribute to the kinetics of nitroso transfer through the results of experimental,[4] ab initio,[5,6] and empirical linear free energy relationship (LFER) studies.[7−10] However, comparatively less work has focused on the thermodynamics of nitroso transfer, although there have been several previous studies on bond dissociation energies.[11]

Nitrosation most commonly proceeds through initial formation of a nitrosating agent of the form ONX, where X is a strong nucleophilic species. Nitrosating agent formation is typically represented by the overall reaction of eq 1, where the nucleophile undergoes reaction with nitrous acid. Under acidic conditions, nitrosating agent formation is usually at equilibrium, with the rate-controlling step being the subsequent reaction of the nitrosating agent with a substrate. However, to determine the intrinsic rate constant for any subsequent reaction steps, we must know the magnitude of the equilibrium constant for nitrosating agent formation, K_{ONX}. For this reason, K_{ONX} values for the formation of most common nitrosating agents have been determined experimentally. The thermodynamics of nitrosating agent formation have been well quantified empirically,[12] a result of the linear relationship between ln K_{ONX} and Edwards' nucleophilic parameter, E_n.[13] This model was derived from a thermodynamic relationship between bonding in the species ON−X and X−X, suggesting that there is some similarity in these bonding mechanisms.

$$HNO_2 + X^- + H^+ \rightleftharpoons ONX + H_2O \qquad (1)$$

Here, we study nitroso bond formation in the common nitrosating agents ONCl, ONBr, N_2O_3, and ONSCN. We chose to study these species as they represent the simplest of the nitroso compounds for which the most experimental thermodynamic information is available. One would fully expect the results obtained for this system to be transferable to any nitroso species, such as those found in the formation of important *N*-nitrosamines or *S*-nitrosothiols. While there have been several previous ab initio studies on nitrosating agent formation,[14] these studies have not made use of higher correlated theoretical methods, or large basis sets, and further high-level calculations are therefore in order.

Computational Procedures

Calculations were performed using a wide range of theoretical techniques. We utilized second-order Møller-Plesset perturbation theory,[15] as well as the DFT method B3LYP.[16] Both methods were used with the aug-cc-pV*n*Z correlation consistent basis sets, for $n = 2$(D), 3(T), and 4(Q). The resultant energies were

* Author to whom correspondence should be addressed. Phone: (+612) 4921 6177. Fax: (+612) 4921 6920. E-mail: Eric.Kennedy@newcastle.edu.au.

† Current address: New Jersey Institute of Technology, Department of Chemistry and Environmental Science, Newark, NJ 07102.

10.1021/jp054266+ CCC: $37.00
Published on Web 02/01/2007

extrapolated to find the complete basis set (CBS) energy, E_∞, using eq 2, where A is an empirical parameter that was fit using a least-squares methodology. Further CBS calculations were performed using the MP4 and QCISD theoretical methods, both with and without triple excitations. These methods provide a better account of multireference character and electron correlation than both the MP2 and the B3LYP methods but at a substantially increased computational cost. Accordingly, these calculations were performed only as single-point energy calculations, using MP2/aug-cc-pVQZ molecular geometries and free energy corrections. The MP2 calculations feature all electrons in the correlation calculation, while the MP4 and QCISD calculations only include the valence electrons.

$$E_\infty = E_n - \frac{A}{(n+1)^4} \tag{2}$$

In addition to the pure ab initio and DFT methods described above, a range of high-accuracy composite techniques were also utilized, namely, G2,[17] G3,[18] G3B3,[19] CBS-Q,[20] and CBS-QB3.[21] Furthermore, we also report G1 and G2MP2 results, which are derivatives of the G2 calculations.

Typically, closed shell calculations were performed, except for potential energy scans, where unrestricted calculations were used. Geometry optimizations were considered to have converged at the following criteria: maximum force = 0.000015, root-mean-square of the force = 0.00001, maximum displacement = 0.00006, root-mean-square of the displacement = 0.00004 (in atomic units). Unless otherwise started, frequency calculations were made on all optimized species, and they were identified to be stable ground state minima by virtue of their lack of any imaginary frequencies. All calculations were performed for solvation in water, with solvent effects described using the default implementation of the polarizable continuum model (PCM). All computations were carried out with the Gaussian 03 suite of programs.[22] A natural bond orbital (NBO) study was also performed, using NBO version 3.1.[23]

Results and Discussion

Heterolytic Bond Dissociation Free Energies. This study investigates the nitrosating agents formed from the nucleophilic species Cl^-, Br^-, NO_2^-, and SCN^-. For these nitrosating agents, the free energy of heterolytic ON−X bond dissociation has been calculated from experimental results according to eq 3, which is derived in Supporting Information. The experimental results (K_{ONX}) used to calculate D_{298}(ON−X) were taken from refs 24 (ONCl and ONBr), 25 (N_2O_3), and 26 (ONSCN). Note that in this contribution we refer to nitroso bond free energies as D_{298}(ON−X), and bond enthalpies and entropies as DH_{298}(ON−X) and DS_{298}(ON−X), respectively.

$$D_{298}(\mathrm{ON-X}) = RT \ln K_{ONX} + 45520 \tag{3}$$

The structure of ONSCN has been investigated previously using ab initio methods,[14b,27] and the nitroso group has been found to bond to the sulfur atom in thiocyanate, in preference to the harder nitrogen site. However, whether ONSCN adopts the cis or the trans conformation has not been studied. In our calculations, different theoretical methods returned different lowest-energy conformers for ONSCN, and in many cases the conformer of higher energy was also found to have a negative imaginary frequency. For the B3LYP method, *cis*-ONSCN was found to be more stable, while for the MP2 method *trans*-ONSCN was more stable. We are therefore unable to identify which is the correct conformation of ONSCN. Furthermore, it is possible that rotation about the ON−SCN bond in nitroso thiocyanate is in fact a free or hindered internal rotor and should therefore not be treated as a vibrational frequency. Such an internal rotor would have a significant effect on the entropy, and therefore free energy, of ONSCN. The internal rotor profile for rotation about the ON−SCN bond has been calculated from a relaxed scan of the corresponding dihedral angle at the B3LYP/6-31G(d) level and is reproduced here as Figure 1. While *cis*-ONSCN is the most stable conformation at this level of theory, *trans*-ONSCN is only around 5 kJ mol^{-1} higher in energy. The barrier for internal rotation about the ON−SCN bond is relatively large, at around 25 kJ mol^{-1}. It is therefore unlikely that the ON−SCN internal rotor is acting as a hindered rotor. Furthermore, at the B3LYP/aug-cc-pVQZ level, the vibrational mode corresponding to ON−SCN internal rotation has a relatively large frequency of 193 cm^{-1}. This further supports our treatment of this vibrational mode as a frequency and not as a hindered internal rotation.

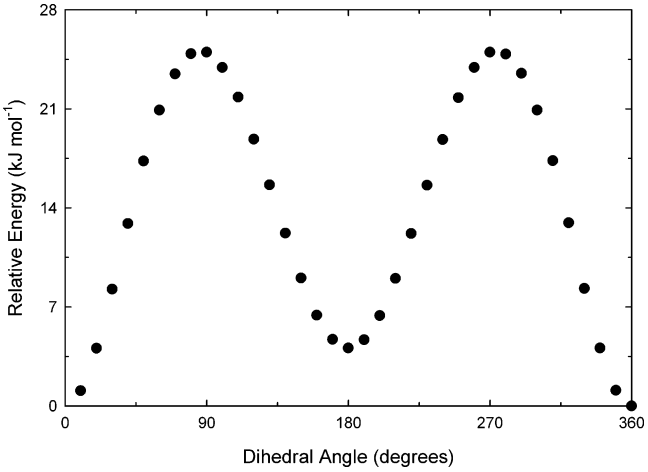

Figure 1. Relaxed potential energy scan of the ON−SCN internal rotor at the B3LYP/6-31G(d) level of theory.

TABLE 1: MP2 ON−X Bond Free Energies (kJ mol^{-1}), with aug-cc-pV*n*Z Basis Sets (n = 2(D), 3(T), 4(Q)), and at the Complete Basis Set (CBS) Limit

	MP2/aug-cc-pVDZ	MP2/aug-cc-pVTZ	MP2/aug-cc-pVQZ	MP2/CBS
ONCl	24.50	32.51	30.88	33.40
ONBr	30.12	40.52	37.18	40.77
N_2O_3	58.01	68.73	64.64	68.51
ONSCN	33.33	40.26	35.93	38.80

The free energy of heterolytic ON−X bond dissociation is calculated from the computed free energy of ONX, ON^+, and X^- according to eq 4. Using the B3LYP and MP2 theoretical methods, we have performed calculations with the correlation-consistent basis sets of Dunning and co-workers, from double- through quadruple-ζ, with diffuse functions added (i.e., aug-cc-pV*n*Z, for n = 1−3), extrapolated to the complete basis set limit. Initially, the MP2 and B3LYP methods were investigated, with geometry optimizations and frequency calculations performed at each level. However, because of memory constraints the very large MP2/aug-cc-pVQZ frequency calculations could not be completed on ONBr, ONSCN, and N_2O_3, and here the aug-cc-pVTZ frequency calculations were used for the free energy corrections, with aug-cc-pVQZ optimized geometries and energies. Tables 1 and 2 list the MP2 and B3LYP bond energies obtained with each of the basis sets, and at the CBS limit, for ONCl, ONBr, N_2O_3, and ONSCN, while Figure 2 shows a plot of the average error at each level of theory. Comparatively, the experimentally derived bond free energies for ONCl, ONBr,

TABLE 2: B3LYP ON−X Bond Free Energies (kJ mol^{-1}), with aug-cc-pV*n*Z Basis Sets (n = 2(D), 3(T), 4(Q)), and at the Complete Basis Set (CBS) Limit

	B3LYP/ aug-cc-pVDZ	B3LYP/ aug-cc-pVTZ	B3LYP/ aug-cc-pVQZ	B3LYP/ CBS
ONCl	88.22	81.00	80.41	78.68
ONBr	93.23	85.51	84.92	83.06
N_2O_3	110.41	104.59	103.81	102.50
ONSCN	98.49	90.44	89.56	87.82

TABLE 3: MP4 and QCISD Bond Free Energies (kJ mol^{-1}) with and without Triples Excitations for ONX Compounds, with aug-cc-pV*n*Z Basis Sets (n = 2−4), and at the Complete Basis Set (CBS) Limit

		aug-cc-pVDZ	aug-cc-pVTZ	aug-cc-pVQZ	CBS
MP4(SDQ)	ONCl	11.54	15.62	13.13	14.85
	ONBr	16.74	20.04	15.92	17.86
	N_2O_3	33.39	38.18	37.66	39.05
	ONSCN	20.65	19.50	17.06	17.40
MP4(SDTQ)	ONCl	34.46	40.70	39.06	41.12
	ONBr	41.08	46.92	43.97	46.27
	N_2O_3	65.36	72.76	73.22	75.04
	ONSCN	45.00	46.20	44.60	45.33
QCISD	ONCl	11.09	15.56	13.15	14.95
	ONBr	16.02	19.67	15.69	17.68
	N_2O_3	27.92	34.10	34.03	35.66
	ONSCN	20.00	19.27	17.14	17.51
QCISD(T)	ONCl	29.06	34.54	32.38	34.37
	ONBr	35.87	40.47	36.83	38.98
	N_2O_3	51.02	57.89	58.15	59.87
	ONSCN	41.31	41.62	39.79	40.35

N_2O_3, and ONSCN are 37.3, 46.8, 58.2, and 62.8 kJ mol^{-1}, respectively.

$$D_{298}(\mathrm{ON{-}X}) = G^{\circ}_{f,\mathrm{ONX}} - G^{\circ}_{f,\mathrm{ON^+}} - G^{\circ}_{f,\mathrm{X^-}} \qquad (4)$$

From the results presented in Tables 1 and 2, and Figure 2, we find that the MP2 method performs well with each basis set, typically showing a small improvement with increasing basis set size, up to the CBS limit. For the B3LYP method, we find good basis set consistency, in that the average error in the calculated bond energies shows a large but diminishing improvement with increasing basis set size. However, the B3LYP bond energies converge toward an average value 37 kJ mol^{-1} above the experimental results, as the B3LYP calculations overestimate the nitroso bond free energy by 30−40 kJ mol^{-1} for every nitrosating agent. This indicates a systematic failure of the B3LYP functional to describe the energy of nitroso species, and we feel that this is an indication that the B3LYP method is incapable of adequately describing the long-range and/or nonbonded component(s) of the ON−X bond energy.

In addition to the MP2/CBS and B3LYP/CBS calculations, we have performed single-point QCISD(T)/CBS calculations (but with the frozen core approximation), using the MP2/aug-cc-pVQZ optimized geometries and frequencies (with aug-cc-pVTZ free energy corrections for the ONSCN, ONBr, and N_2O_3 geometries). Additionally, we also report the intermediate MP4(SDTQ) bond energies, as well as the MP4(SDQ) and QCISD results, i.e., MP4(SDTQ) and QCISD(T) without triples excitations. Table 3 presents the bond energies at each level of theory, with the average error for the four calculation schemes plotted in Figure 3 as a function of basis set size. We find that the best results are provided by QCISD(T) and MP4(SDTQ), which offer only a small improvement (ca. 3−5 kJ mol^{-1}) over the MP2 results. However, it is important to note that the MP2 calculations included all electrons in the correlation calculation, while

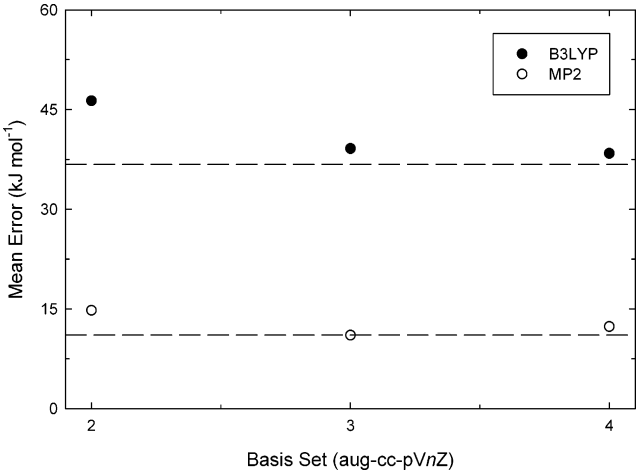

Figure 2. Plot of average absolute error versus basis set size, for B3LYP and MP2 ON−X bond free energies, with aug-cc-pV*n*Z basis sets (n = 2−4) and at the complete basis set (CBS) limit (denoted by dashed lines).

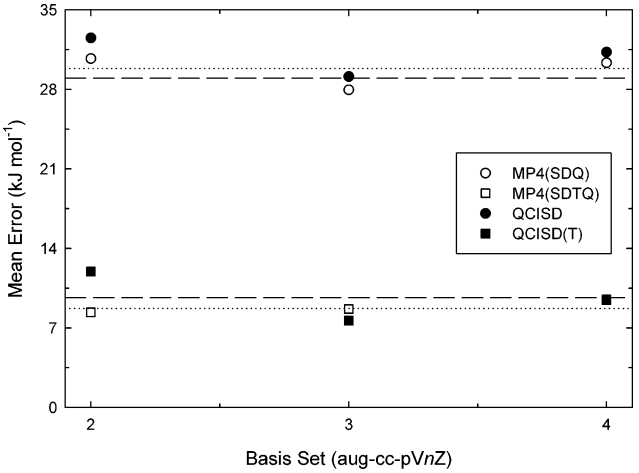

Figure 3. Plot of average error versus basis set size, for MP4(SDQ), MP4(SDTQ), QCISD, and QCISD(T) ON−X bond free energies, with aug-cc-pV*n*Z basis sets (n = 2−4), and at the complete basis set (CBS) limit (denoted by dashed lines for MP4 and dotted lines for QCISD).

the QCISD(T) calculations only included the valence electrons. At the CBS limit, the QCISD(T) calculations provide a small advantage relative to the MP4(SDTQ) calculations; however, it is difficult to justify the increased computational expense of the QCISD(T) method over MP4(SDTQ) based upon this result. Additionally, for all calculations, the aug-cc-pVTZ basis set provided smaller errors than the aug-cc-pVQZ basis set. Finally, we feel that the most important result that can be drawn from the QCISD(T) calculations is that the inclusion of triple excitations are necessary to obtain accurate bond energies, with the addition of triples to the MP4 and QCISD calculations found to yield an increase in accuracy of around 20 kJ mol^{-1}.

The free energy of ON−X bond dissociation has been calculated using seven composite theoretical methods, and the calculated bond energies are compared to experimental results in Table 4. Also included in Table 4 is the average absolute error for each method relative to the experimental values. Many of the composite theoretical methods used here were recently applied with considerable success to calculate the acidity of the nitrosation reagent nitrous acid, in the gas and liquid phases,[28] and we expect them to provide relatively accurate nitroso bond energies without the large computational requirements of the CBS calculations detailed above.

TABLE 4: Predicted Free Energies of ON−X Bond Dissociation for Seven Composite Theoretical Methods, Compared to Experimental Values[a]

	D_{298}(ON−X) (kJ mol^{-1})							
	expt	G2	G2MP2	G1	G3	G3B3	CBS-Q	CBS-QB3
ONCl	37.3	41.6	41.5	49.8	45.7	36.5	37.4	31.6
ONBr	46.8	45.1	44.7	47.1	49.0	41.6	47.4	41.0
N_2O_3	58.2	54.8	55.8	58.8	59.9	60.6	60.2	59.1
ONSCN	62.8	55.6	58.1	64.8	56.2	46.1	53.0	51.2
error		4.2	3.4	3.9	4.7	6.3	3.1	6.0

[a] All values in kJ mol^{-1}.

TABLE 5: Values of the Q_1 Multireference Character Diagnostic, from QCISD(T)/aug-cc-pVDZ Calculations

	Q_1
ON^+	0.0156
Cl^-	0.0049
Br^-	0.0035
NO_2^-	0.0235
SCN^-	0.0122
ONCl	0.0159
ONBr	0.0134
N_2O_3	0.0212
ONSCN	0.0172

We find in Table 4 that all of the compound methods provide accurate predictions of the bond free energies. The CBS-Q method is the most successful, followed by the G2MP2, G2, and G1 methods. The average errors obtained with these four methods are smaller than those for the G2 molecule test-set, which is an especially pleasing result given the additional error in our calculations, over those of the G2 test-set, arising from the inclusion of a solvent. The remaining composite methods (G3, G3B3, and CBS-QB3) all predict the experimental results to within good accuracy, although the errors are slightly greater than those for the G2 molecule test-set. Comparatively, all of the composite methods yield more accurate results than the much more computationally intensive QCISD(T)/CBS calculations. Also, while we earlier found the B3LYP method to be inadequate at describing the energy of nitroso compounds, it appears as though this DFT method is relatively adept at predicting the structure of nitroso species, based upon the similar results of the G3 and G3B3 and the CBS-Q and CBS-QB3 calculations.

The largest average error of any one nitrosating agent with the composite theoretical calculations was for ONSCN. We also find above that ONSCN is the worst performed nitrosating agent with the QCISD(T)/CBS calculations, where the error is 22.45 kJ mol^{-1}. This perhaps reflects the difficulty in locating this species' correct ground-state conformation and/or correctly treating the ON−SCN internal rotor but could also indicate that this molecule possesses significant multireference character. To investigate the possible importance of multireference character, we have calculated the Q_1 diagnostic,[29] which is obtained from QCISD single excitation amplitudes, at the QCISD(T)/aug-cc-pVDZ level of theory. Calculated Q_1 values for all species are listed in Table 5. We find that Q_1 is actually relatively small for ONSCN and SCN^-, and it is therefore unlikely that there is significant multireference character in either of these molecules. The largest values for Q_1 are obtained with NO_2^- and N_2O_3. However, the N_2O_3 ON−X bond energy is accurately reproduced at most levels of theory, indicating that multireference character is still not overly significant or that there is good cancellation of the error induced by multireference character across the bond dissociation reaction.

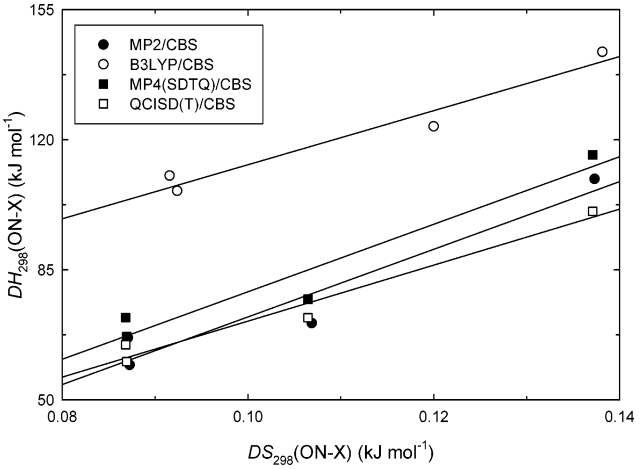

Figure 4. Enthalpy−entropy compensation diagram for ON−X bond dissociation, with four theoretical methods.

TABLE 6: Nitrosating Agent Structures Optimized at the MP2/aug-cc-pVQZ and B3LYP/aug-cc-pVQZ Levels of Theory[a]

	ON−X		O═N		∠ O═N−X	
	MP2	B3LYP	MP2	B3LYP	MP2	B3LYP
ONCl	2.1489	2.1277	1.1123	1.1055	113.17	113.82
ONBr	2.2607	2.2667	1.1184	1.1095	114.55	114.96
N_2O_3	1.8349	1.9031	1.1390	1.1181	105.18	106.10
ONSCN[b]	2.2086	2.1489	1.1218	1.1212	116.29	115.23

[a] Bond lengths are in angstroms, and angles are in degrees. [b] *cis*-ONSCN for MP2 and *trans*-ONSCN for B3LYP.

Using each of the above ab initio, DFT and composite theoretical methods, ON−X bond enthalpies and entropies (DH_{298}(ON−X) and DS_{298}(ON−X)) have been determined, using the same methodology as for the bond free energies. These values are provided in Supporting Information. Figure 4 shows the enthalpy−entropy compensation relationship (or isoequilibrium relationship)[30] between DH_{298}(ON−X) and DS_{298}(ON−X) for the MP2/CBS, MP4(SDTQ)/CBS, QCISD(T)/CBS, and B3LYP/CBS results. We find that, in general, a good linear relationship exists, with an average slope, or isoequilibrium temperature, of 825 ± 98 K across all four methods. Considering that $\Delta G = \Delta H - T\Delta S$, dividing the obtained slope by T yields the relative effects of enthalpy and entropy on the free energy. Accordingly, the effects of enthalpy are over two times as important as entropy on the free energy of ON−X bond dissociation. The calculated isoequilibrium temperature of 841 K is among the largest observed for an enthalpy−entropy relationship (cf. Leffler and Grunwald[31]), indicating the extent to which enthalpic effects dominate over entropic effects. We also observe in Figure 4 that, while the B3LYP method predicts entropy values to be qualitatively similar to those of the other, more accurate, methods, it routinely overpredicts the enthalpy values by around 40 kJ mol^{-1}. This deviation corresponds to the error observed for the B3LYP free energies, and thus we can conclude that the error in the B3LYP bond free energies arises almost entirely from the error associated with estimation of the molecular enthalpies and not entropies. Entropy values are calculated according to statistical mechanical principles from geometrical and vibrational parameters, and these results therefore validate our earlier assertion that the B3LYP method provides an accurate account of the geometry and frequencies of nitroso compounds.

Nitrosating Agent Structure. Table 6 lists the optimized ON−X and O═N bond lengths, and the O═N−X angles, for the four studied nitrosating agents at the MP2/aug-cc-pVQZ and

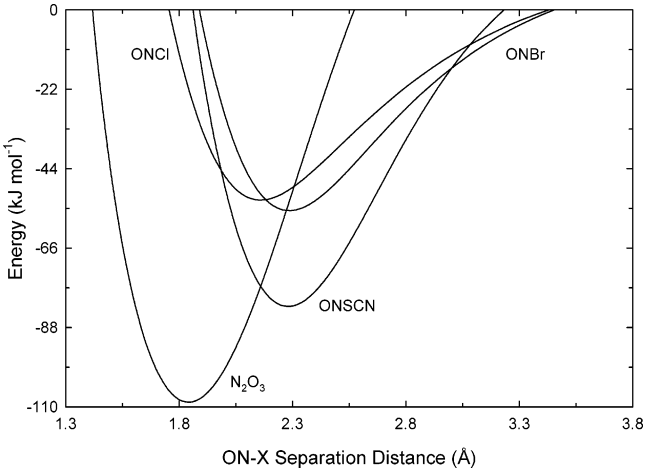

Figure 5. Relaxed potential energy scans of the ON−X bond in four nitrosating agents, at the UMP2(full)/6-311+G(3df) level of theory.

B3LYP/aug-cc-pVQZ levels. Both theoretical methods return similar results for all four nitrosating agents, which supports our earlier finding that the B3LYP functional can accurately predict the structure of nitroso species. From Table 6, the O═N bond length is predicted to vary little between nitrosating agents, even though the four nucleophiles studied cover a wide range of nucleophilic reactivity. Additionally, the O═N−X bond angles are all relatively similar, except that of N_2O_3, which is on average around 10° more acute than the others. The ON−X bonds are all around 2 Å, which is unusually long for a covalent single bond. The length of the ON−X bond also shows considerable variation from one nitrosating agent to the other, covering a range of over 0.4 Å. Although not included in the table, the linear structure of the thiocyanate ion was predicted to be distorted by around 5° toward the nitroso group in *cis*-ONSCN.

Nitrosating Agent Bonding. To observe the interrelationship between bond energy and bond length, relaxed potential energy scans were performed at the MP2/6-311+G(3df) level for the ON−X bonds in each of the four nitrosating agents, and the results are shown here in Figure 5. In constructing Figure 5, an energy of zero was arbitrarily assigned to the structure obtained at an infinite separation distance, to ensure that any activation barrier was not incorporated into the depth of the potential energy well. We find that there is no real correlation between the depth of a potential energy well and the well's location.

From Figure 5 we find that while the energy of a nitrosating agent decreases with increasing nucleophilic strength, the nitroso bond length does not. This relates to our earlier observation of a large isoequilibrium temperature from the enthalpy−entropy compensation diagram, which we concluded was a result of entropy effects being less significant than enthalpy effects. Enthalpy−entropy compensation is thought to arise because of the effect of a species' energy (closely related to enthalpy) upon its structure (closely related to entropy).[35] For instance, by increasing the strength of a covalent bond in a molecule, we would expect to observe a decrease in the molecule's enthalpy. However, it is well-known that as the strength of a bond increases, there is typically a compensatory decrease in the length of the bond, thus imparting increased order (i.e., decreased entropy) upon the molecule. As a result, a decrease in enthalpy can be expected to result in a decrease in entropy, as is often observed experimentally. However, in our instance we find that a large change in enthalpy results in only a relatively minor (though linearly proportional) change in entropy.

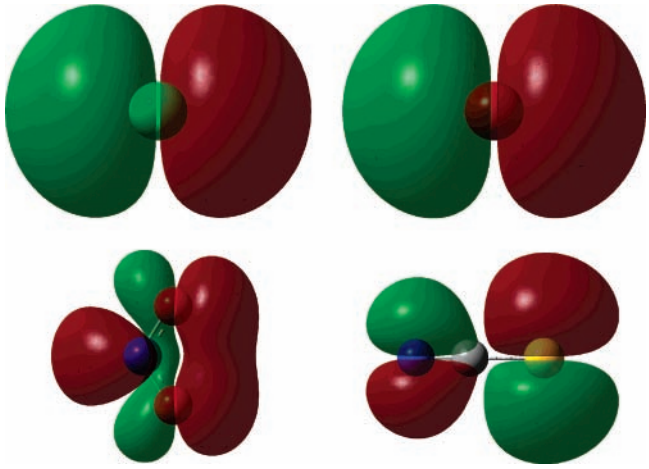

Figure 6. Highest occupied molecular orbitals (HOMOs) for Cl^-, Br^-, NO_2^-, and SCN^-, respectively.

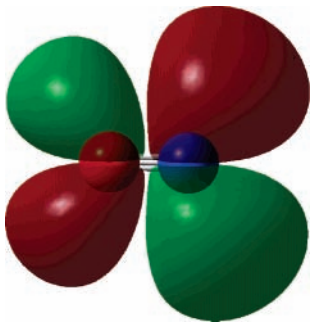

Figure 7. Lowest unfilled molecular orbital (LUMO) for ON^+.

A possible explanation for this lack of correlation between bond length and bond energy is the resonance stabilization that occurs in N_2O_3, and to a lesser extent in ONSCN, due to the π-electron donating properties of the NO_2^- and SCN^- groups. While resonance stabilization may significantly alter the nitrosating agent structure by shortening the ON−X bond length, it has little effect on the molecule's energy. This follows as a corollary of our enthalpy−entropy relationship, as large entropic changes have only small enthalpic ramifications. If, in Figure 5, the ON−X bond length was increased significantly in N_2O_3, and less significantly in ONSCN, then we would begin to see some degree of correlation between the depth and the location of the potential energy wells.

We have constructed molecular orbital diagrams so as to further our understanding of the bonding in each of the nitrosating agents. In addition, a natural bond orbital analysis has been performed for each nitrosating agent to help interpret the visualized molecular orbitals. Figure 6 shows the highest occupied molecular orbitals (HOMOs) for each of the nucleophilic species, while the lowest unfilled molecular orbital (LUMO) for ON^+ is depicted in Figure 7. The HOMOs for the four nitrosating agents are provided in Figure 8. In all cases, the molecules are oriented with the *z*-axis perpendicular to the plane of the paper, with the *x*-axis extending horizontally.

The LUMO for ON^+ (Figure 7) consists of an unoccupied π antibonding orbital (π^*) (the ON^+ HOMO is a π bonding orbital). The NBO analysis predicts a Lewis structure for ON^+ with three bonding electron pairs and lone pairs on the oxygen and nitrogen atoms. The NBO calculations also found each of oxygen's 2p orbitals to contain 1.33 electrons, while nitrogen's 2p orbitals contained only 0.65 electrons each, explaining why the positive charge of ON^+ is located primarily on the nitrogen atom.

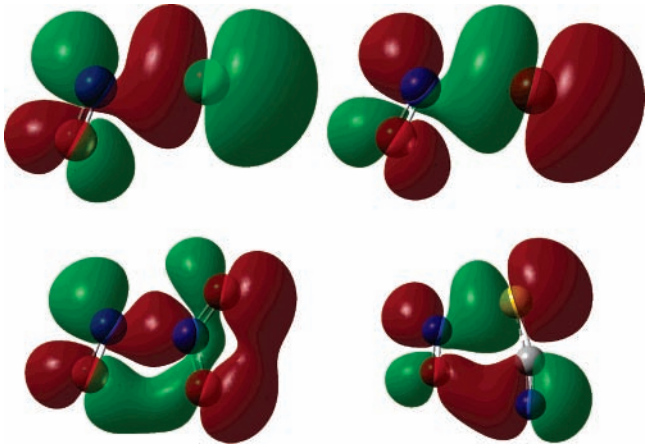

Figure 8. Highest occupied molecular orbitals (HOMOs) for ONCl, ONBr, N_2O_3, and ONSCN, respectively.

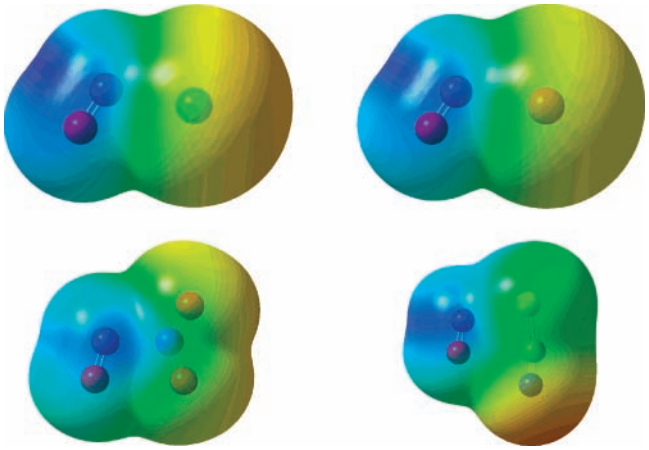

Figure 9. Electrostatic potential mapped onto electron density for ONCl, ONBr, N_2O_3, and ONSCN, respectively. Electrostatic potential ranges from -8.255×10^{-2} (red) to 8.255×10^{-2} (blue).

For bonding of ON^+ with the two halide ions, an electron from the halide's full HOMO, consisting of predominantly p_x orbital contributions, is shared with the unoccupied π^* orbital of ON^+, thus creating the filled molecular orbitals seen in Figure 8 for ONCl and ONBr. From the NBO calculations, the highest energy valence atomic orbitals for the halide atoms in ONCl and ONBr were the $3p_x$ and $4p_x$ orbitals respectively, as would be expected. Each of these respective orbitals was found to be occupied by 1.62 and 1.56 electrons each, therefore decreasing with decreasing bond free energy. Both nitrosating agents were predicted to share the same Lewis structure, with three bonding electron pairs and six lone pairs (two on the oxygen atom, one on the nitrogen, and three on the halide).

Formation of ONSCN is quite different from formation of the nitrosyl halides, because the HOMO of SCN^- resembles the π^* LUMO of ON^+. The main orbital overlap is similar to that for the nitrosyl halides, with one of the electrons from the SCN^- HOMO being shared with the ON^+ π^* LUMO. NBO analysis indicates that the nitroso oxygen atom is predominantly undergoing π bonding with the thiocyanate carbon atom, through their adjacent 2p valence orbitals. However, bonding also occurs between the nitroso oxygen and the cyano group, forming a second, weaker covalent bond. This bond is responsible for distorting the linear geometry of the thiocyanate group in *cis*-ONSCN. The added stability afforded by the O−C bond explains why *cis*-ONSCN may be more stable than *trans*-ONSCN. However, this bond also acts to destabilise *cis*-ONSCN over *trans*-ONSCN, due to the close proximity of the antibonding lobes shared by the N−S and the O−C groups. In *trans*-ONSCN, the more relaxed geometry allows for a greater separation distance between these antibonding orbitals, thus lowering the molecule's energy. The combination of the above two factors explains why there is only a small energy difference between *trans*- and *cis*-ONSCN, and why the actual conformation of ONSCN is difficult to unequivocally determine.

The bonding in N_2O_3 is also complicated, due to the significant π resonance of the nitro group. In Figure 8, one of the nitrogen atoms in the nitrite group appears to bond with the nitroso nitrogen π^* orbital, where the bonding components from the nitro nitrogen are mainly s and p atomic orbitals. However, the corresponding p atomic orbitals, of opposite sign, on the nitro oxygen atoms result in a π bond, which undergoes bonding with the nitroso oxygen atom. The electron pair resonating between these atoms may undergo bonding with the adjacent lobe of the ON^+ π^* orbital, as their wavefunctions are of the same sign (phase). The resulting bond is responsible for the more acute O═N−X angle and shorter ON−X bond length observed in N_2O_3 versus the other nitrosating agents. While this extra bonding interaction is responsible for significantly shortening the ON−NO_2 bond, it has little effect on the overall bond energy. One contribution to this effect would be the bringing together of two antibonding orbitals, as was found for *cis*-ONSCN.

We have constructed electron density surfaces for the four nitrosating agents, onto which the electrostatic potential has been mapped, as illustrated in Figure 9. Generally, with increasing E_n of the nucleophile we find that the positive charge on the nitroso group decreases, due to increased electron sharing resulting from the stronger covalent bond. However, the order of N_2O_3 and ONSCN does appear to be the reverse of what we would expect from the respective E_n values of their constituent nucleophiles. In ONSCN, we see that the nitrogen atom in thiocyanate is much more electronegative than the sulfur atom, which is in accordance with the observation that the nitrogen atom provides a hard reaction site, while the sulfur atom provides a soft reaction site. Furthermore, we find that this hard nitrogen atom in ONSCN is the most electronegative site in any of the nitrosating agents. It is therefore plausible that significant hydrogen bonding (a hard−hard interaction) could take place at this nitrogen atom. Strong hydrogen bonds are poorly described by continuum solvent models, and this could explain the relatively poor bond energies calculated for ONSCN. To test this hypothesis, one would need to calculate the bond energy of ONSCN using either a discrete or a hybrid discrete-continuum solvent model, where individual water molecules are included in the calculations, bonded to the solute.

Conclusion

We present one of the first studies on bonding in nitroso species using high-level ab initio techniques. Nitroso species represent a diversely important group of compounds, and we have made several important discoveries relating to the nature of nitroso bonding. Our conclusions are as follows:

(1) Compound ab initio techniques such as G2 and CBS-QB3 can accurately predict nitroso bond free energies. MP2/CBS calculations provide a relatively good account of the nitroso bond energy, with a small improvement made by moving to MP4(SDTQ)/CBS and QCISD(T)/CBS calculations. However, the inclusion of triple excitations is required to achieve this improvement. The B3LYP density functional method systematically fails to accurately calculate nitroso bond energies, overpredicting the values by ca. 40 kJ mol^{-1} at the CBS limit.

(2) The enthalpy of ON−X bond dissociation is linearly proportional to the entropy of ON−X bond dissociation, due to enthalpy−entropy compensation. The slope of this enthalpy−entropy compensation relationship was large (825 K), indicating that the contribution of enthalpy to free energy is greater than that of entropy. Enthalpy−entropy compensation also revealed that the B3LYP functional accurately predicts nitroso bond entropy but overpredicts the bond enthalpy by around 40 kJ mol^{-1}.

(3) Molecular orbital diagrams illustrated that nitroso bonding takes place due to overlap of the ON^+ LUMO with the HOMO of the nucleophile, where the LUMO of ON^+ is a π antibonding orbital. Bonding is similar in each of the nitrosyl halides, although for ONSCN and N_2O_3 the nitroso oxygen appears to undergo some degree of bonding with the nucleophile. Further insight into the mechanism of bonding was obtained through NBO analysis and by studying electrostatic potential surfaces.

Acknowledgment. We would like to acknowledge the financial support of the Australian Research Council and Orica Australia.

Supporting Information Available: Derivation of a thermodynamic relationship between ON−X bond free energy and K_{ONX}. Enthalpy and entropy of ON−X bond dissociation. This material is available free of charge via the Internet at http://pubs.acs.org.

References and Notes

(1) (a) Butler, A. R.; Williams, D. L. H. *Chem. Soc. Rev.* **1993**, 233. (b) Calver, A.; Collier, J.; Vallance, P. *Environ. Physiol.* **1993**, *78*, 303. (c) Frey, A.; Reif, A.; Zabel, U.; Schmidt, H. *BIOspektrum* **1998**, *4*, 27. (d) Nathan, C.; Xie, Q. W. *Biol. Chem.* **1994**, *269*, 13725.

(2) (a) Magee, P. N.; Barnes, J. M. *Brit. J. Cancer* **1956**, *10*, 114. (b) Mirvish, S. S. *Cancer Lett.* **1995**, *93*, 17. (c) Shephard, S. E.; Lutz, W. K. *Cancer Surv.* **1989**, *8*, 401.

(3) (a) da Silva, G.; Dlugogorski, B. Z.; Kennedy, E. M. *AIChE J.* **2006**, *52*, 1558. (b) da Silva, G.; Dlugogorski, B. Z.; Kennedy, E. M. *Int. J. Chem. Kin.* **2006**, manuscript submitted. (c) Nguyen, D. A.; Iwaniw, M. A.; Fogler, H. S. *Chem. Eng. Sci.* **2003**, *58*, 4351.

(4) (a) Adam, C.; García-Río, L.; Leis, J. R. *Org. Biomol. Chem.* **2004**, *2*, 1181. (b) Boni, J. C.; García-Río, L.; Leis, J. R.; Moreira, J. A. *J. Org. Chem.* **1999**, *64*, 8887. (c) Darbeau, R. W.; Pease, R. S.; Perez, E. V. *J. Org. Chem.* **2002**, *67*, 2942. (d) García-Río, L.; Leis, J. R.; Moreira, J. A.; Serantes, D. *Eur. J. Org. Chem.* **2004**, 614.

(5) (a) Gwaltney, S. R.; Rosokha, S. V.; Head-Gordon, M.; Kochi, J. K. *J. Am. Chem. Soc.* **2003**, *125*, 3273. (b) Leach, A. G.; Houk, K. N. *Org. Biomol. Chem.* **2003**, *1*, 1389. (c) Reynolds, C. A.; Thomson, C. *J. Chem. Soc. Perkin Trans. 2* **1987**, 1337. (d) Skokov, S.; Wheeler, R. A. *J. Phys. Chem. A* **1999**, *103*, 4261.

(6) da Silva, G.; Dlugogorski, B. Z.; Kennedy, E. M. *Chem. Eng. Sci.* **2006**, *61*, 3186.

(7) da Silva, G.; Kennedy, E. M.; Dlugogorski, B. Z. *Ind. Eng. Chem. Res.* **2004**, *43*, 2296.

(8) da Silva, G.; Kennedy, E. M.; Dlugogorski, B. Z. *J. Phys. Org. Chem.* **2006**, in press.

(9) da Silva, G.; Kennedy, E. M.; Dlugogorski, B. Z. *J. Am. Chem. Soc.* **2005**, *127*, 3664.

(10) (a) García-Río, L.; Leis, J. R.; Moreira, J. A.; Norberto, F. *J. Chem. Soc. Perkin Trans. 2* **1998**, 1613. (b) García-Río, L.; Leis, J. R.; Moreira, J. A.; Norberto, F. *J. Org. Chem.* **2001**, *66*, 381. (c) Leis, J. R.; Peña, M. E.; Ríos, A. M. *J. Chem. Soc. Perkin Trans. 2* **1995**, 587. (d) Leis, J. R.; Ríos, A.; Rodríguez-Sánchez, L. *J. Chem. Soc. Perkin Trans. 2* **1998**, 2729. (e) Munro, A. P.; Williams, D. L. H. *J. Chem. Soc. Perkin Trans. 2* **1999**, 1989.

(11) (a) Bartberger, M. D.; Mannion, J. D.; Powell, S. C.; Stamler, J. S.; Houk, K. N.; Toone, E. J. *J. Am. Chem. Soc.* **2001**, *123*, 8868. (b) Bartsch, R. A.; Chae, Y. M.; Ham, S.; Birney, D. M. *J. Am. Chem. Soc.* **2001**, *123*, 7479. (c) Cheng, J.; Xian, M.; Wang, K.; Zhu, X.; Yin, Z.; Wang, P. G. *J. Am. Chem. Soc.* **1998**, *120*, 10266. (d) Fu, Y.; Mou, Y.; Lin, B.; Liu, L.; Guo, Q. *J. Phys. Chem. A* **2002**, *106*, 12386. (e) Lü, J.; Wittbrodt, J. M.; Wang, K.; Wen, Z.; Schlegel, B.; Wang, P. G.; Cheng, J. *J. Am. Chem. Soc.* **2001**, *123*, 2903. (f) Zhu, X.; He, J.; Li, Q.; Xian, M.; Lu, J.; Cheng, J. *J. Org. Chem.* **2000**, *65*, 6729.

(12) da Silva, G.; Kennedy, E. M.; Dlugogorski, B. Z. *J. Chem. Res.* **2002**, 589.

(13) Edwards, J. O. *J. Am. Chem. Soc.* **1954**, *76*, 1540.

(14) (a) Jørgensen, K. A.; El-Wassimy, M. T. M.; Lawesson, S. O. *Acta Chem. Scand.* **1983**, *B37*, 785. (b) Jørgensen, K. A.; Lawesson, S. O. *J. Chem. Soc. Perkin Trans. 2* **1985**, 231. (c) Nguyen, M. T.; Hegarty, A. F. *J. Chem. Soc. Perkin Trans. 2* **1984**, 2037. (d) Reynolds, C. A.; Thomson, C. *J. Chem. Soc. Perkin Trans. 2* **1987**, 1337.

(15) Møller, C.; Plesset, M. S. *Phys. Rev.* **1934**, *46*, 618.

(16) (a) Becke, A. D. *Phys. Rev. A* **1988**, *38*, 3098. (b) Lee, C.; Yang, W.; Parr, R. G. *Phys. Rev. B* **1988**, *37*, 785.

(17) Curtiss, L. A.; Raghavachari, K.; Trucks, G. W.; Pople, J. A. *J. Chem. Phys.* **1991**, *94*, 7221.

(18) Curtiss, L. A.; Raghavachari, K.; Redfern, P. C.; Rassolov, V.; Pople, J. A. *J. Chem. Phys.* **1998**, *109*, 7764.

(19) Baboul, A. G.; Curtiss, L. A.; Redfern, P. C.; Raghavachari, K. *J. Chem. Phys.* **1999**, *110*, 7650.

(20) Ochterski, J. W.; Petersson, G. A.; Montgomery, J. A. *J. Chem. Phys.* **1996**, *104*, 2598.

(21) (a) Montgomery, J. A.; Frisch, M. J.; Ochterski, J. W.; Petersson, G. A. *J. Chem. Phys.* **1999**, *110*, 2822. (b) Montgomery, J. A.; Frisch, M. J.; Ochterski, J. W.; Petersson, G. A. *J. Chem. Phys.* **2000**, *112*, 6532.

(22) Frisch, M. J.; Trucks, G. W.; Schlegel, H. B.; Scuseria, G. E.; Robb, M. A.; Cheeseman, J. R.; Montgomery, Jr., J. A.; Vreven, T.; Kudin, K. N.; Burant, J. C.; Millam, J. M.; Iyengar, S. S.; Tomasi, J.; Barone, V.; Mennucci, B.; Cossi, M.; Scalmani, G.; Rega, N.; Petersson, G. A.; Nakatsuji, H.; Hada, M.; Ehara, M.; Toyota, K.; Fukuda, R.; Hasegawa, J.; Ishida, M.; Nakajima, T.; Honda, Y.; Kitao, O.; Nakai, H.; Klene, M.; Li, X.; Knox, J. E.; Hratchian, H. P.; Cross, J. B.; Adamo, C.; Jaramillo, J.; Gomperts, R.; Stratmann, R. E.; Yazyev, O.; Austin, A. J.; Cammi, R.; Pomelli, C.; Ochterski, J. W.; Ayala, P. Y.; Morokuma, K.; Voth, G. A.; Salvador, P.; Dannenberg, J. J.; Zakrzewski, V. G.; Dapprich, S.; Daniels, A. D.; Strain, M. C.; Farkas, O.; Malick, D. K.; Rabuck, A. D.; Raghavachari, K.; Foresman, J. B.; Ortiz, J. V.; Cui, Q.; Baboul, A. G.; Clifford, S.; Cioslowski, J.; Stefanov, B. B.; Liu, G.; Liashenko, A.; Piskorz, P.; Komaromi, I.; Martin, R. L.; Fox, D. J.; Keith, T.; Al-Laham, M. A.; Peng, C. Y.; Nanayakkara, A.; Challacombe, M.; Gill, P. M. W.; Johnson, B.; Chen, W.; Wong, M. W.; Gonzalez, C.; Pople, J. A. *Gaussian 03, Revision B.05*; Gaussian, Inc.: Pittsburgh, PA, 2003.

(23) Glendening, E. D.; Reed, A. E.; Carpenter, J. E.; Weinhold, F. *NBO Version 3.1*; Theortetical Chemistry Institute: University of Wisconsin, Madison, WI, 1993.

(24) Schmid, H.; Hallaba, E. *Monatsh. Chem.* **1956**, *87*, 560.

(25) Markovits, G. Y.; Schwartz, S. E.; Newman, L. *Inorg. Chem.* **1981**, *20*, 445.

(26) Stedman, G.; Whincup, P. A. E. *J. Chem. Soc.* **1963**, 5796.

(27) (a) Joergensen, K. A.; Lawesson, S. O. *J. Am. Chem. Soc.* **1984**, *106*, 4687. (b) Pasinszki, T.; Westwood, N. P. C. *J. Chem. Soc. Faraday Trans.* **1996**, *92*, 333.

(28) da Silva, G.; Kennedy, E. M.; Dlugogorski, B. Z. *J. Phys. Chem. A* **2006**, *110*, 11371.

(29) Lee, T. J.; Rendell, A. P.; Taylor, P. R. *J. Phys. Chem.* **1990**, *94*, 5463.

(30) (a) Leffler, J. E. *J. Org. Chem.* **1955**, *20*, 1202. (b) Liu, L.; Guo, Q.-X. *Chem. Rev.* **2001**, *101*, 673.

(31) Leffler, J. E.; Grunwald, E. *Rates and Equilibria of Organic Reactions*; John Wiley and Sons: New York, 1963; pp 327−341.